Bioconjugate Chemistry

Article

pubs.acs.org/bc

Optimization of Multivalent Bispecific Antibodies and Immunocytokines with Improved in Vivo Properties

Edmund A. Rossi,*[,†,§] Chien-Hsing Chang,[†,§] Thomas M. Cardillo,[§] and David M. Goldenberg[†,§,‡]

[†]IBC Pharmaceuticals, Inc., Morris Plains, New Jersey, United States

[§]Immunomedics, Inc., Morris Plains, New Jersey, United States

[‡]Garden State Cancer Center, Center for Molecular Medicine and Immunology, Morris Plains, New Jersey, United States

Supporting Information

ABSTRACT: Multifunctional antibody-based biologics, such as bispecific antibodies and immunocytokines, can be difficult to produce with sufficient yield and stability, and often exhibit inferior pharmacokinetics. Dock-and-Lock (DNL) is a modular method that combines recombinant engineering with site-specific conjugation, allowing the construction of various complex, yet defined, biostructures with multivalency and multispecificity. The technology platform exploits the natural interaction between two interactive human protein binding domains that are modified to provide covalent fusion. We explored the potential application of a new class of IgG-based DNL modules with an anchor domain fused at the C-terminal end of the kappa light chain (C_k), instead of the C-terminal end of the Fc. Two C_k-derived prototypes, an anti-CD22/CD20 bispecific hexavalent antibody, comprising epratuzumab (anti-CD22) and four Fabs of veltuzumab (anti-CD20), and a CD20-targeting immunocytokine, comprising veltuzumab and four molecules of interferon-α2b, were compared to their Fc-derived counterparts. The Ck-based conjugates exhibited superior Fc-effector functions in vitro, as well as improved pharmacokinetics, stability, and anti-lymphoma activity in vivo. These results favor the selection of DNL conjugates with the C_k-design for future clinical development.

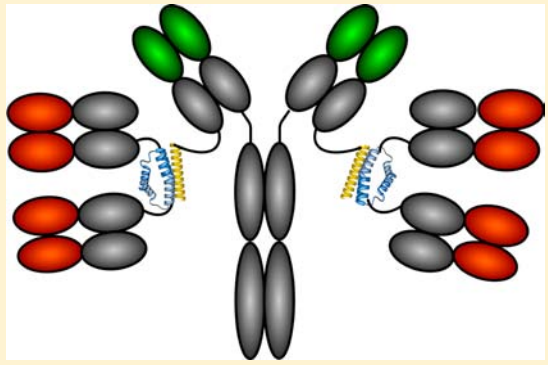

Biomedical research is trending toward the development of increasingly sophisticated antibody-based biologics, such as bispecific antibodies, immunocytokines, and antibody−drug conjugates. The development of more complex, and less natural, fusion proteins is challenged by problems with yield, stability, immunogenicity, and pharmacokinetics (PK). In particular, immunoconjugates based on antibody fragments, including single-chain Fv (scFv), Fab, or other Fc-lacking formats,[1] are often difficult to produce with homogeneity and sufficient yield, lack Fc-effector functions, and inherently suffer from short circulating serum half-lives ($T_{1/2}$). Immunoconjugates of IgG can be produced in high yields, with longer $T_{1/2}$ and in vivo stability. Further, intact monoclonal antibodies (mAbs) offer high-avidity bivalent binding with Fc-effector functions, including antibody-dependent cell-mediated cytotoxicity (ADCC) and complement-dependent cytotoxicity (CDC). The enhanced PK of IgG is attributed to two major factors. Its larger molecular size (~150 kDa) precludes renal clearance, which is responsible for the rapid elimination of smaller constructs (<60 kDa), such as scFv, and its dynamic binding to the neonatal Fc receptor (FcRn)[2] extends $T_{1/2}$.

We have developed the Dock-and-Lock (DNL) method to produce a variety of immunoconjugates in assorted formats.[3] The DNL method utilizes the naturally occurring protein/protein interaction between type II regulatory subunits (RII) of cAMP-dependent protein kinase and the anchor domain (AD) of A-kinase anchor proteins (AKAPs).[4,5] The AD of AKAPs are amphipathic helices of 14−18 residues,[6] which bind specifically to a hydrophobic surface formed by dimeric RII.[7] The dimerization domain and AKAP docking domain are both located in the 44 amino-terminal residues of human RII, which is referred to as the dimerization and docking domain (DDD).[8,9]

Previously, bispecific hexavalent antibodies (bsHexAbs) based on veltuzumab (anti-CD20) and epratuzumab (anti-CD22) were constructed by combining a stabilized $(Fab)_2$ fused with a dimerization and docking domain (DDD) with an IgG containing an anchor domain (AD) appended at the C-terminus of each heavy chain (C_H3-AD2-IgG).[10] Compared to mixtures of their parental mAbs, these Fc-based bsHexAbs, referred to henceforth as "Fc-bsHexAbs", induced unique signaling events[11] and exhibited potent cytotoxicity in vitro. However, the Fc-bsHexAbs cleared from circulation of mice approximately twice as rapidly as the parental mAbs.[10] Although the Fc-bsHexAbs are considerably stable ex vivo,[10] we suspected that some dissociation occurs in vivo, presumably by intracellular processing. Further, the Fc-bsHexAbs lack CDC activity.[10]

Received: August 30, 2012
Revised: October 31, 2012
Published: November 1, 2012

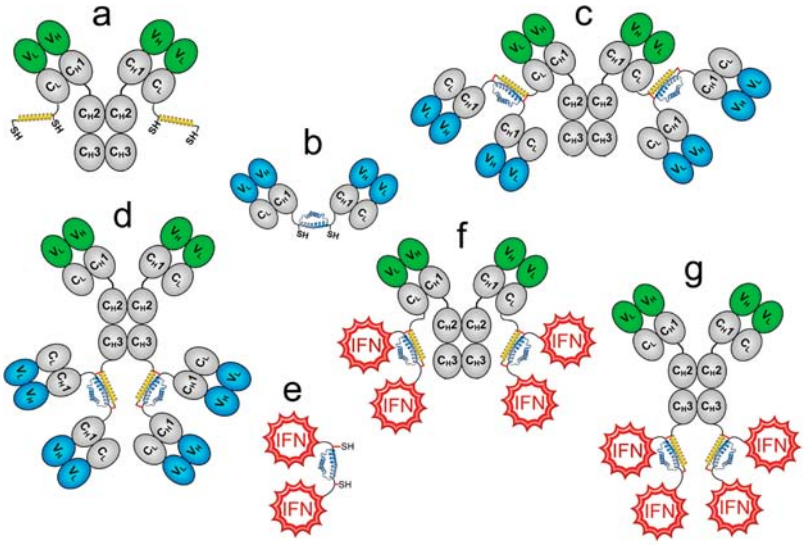

Figure 1. DNL modules and conjugates: (a) C_k-AD2-IgG (C_k-AD2-IgG-epratuzumab or C_k-AD2-IgG-veltuzumab), an IgG-AD2 module with an AD2 fused to the carboxyl-terminal end of each kappa light chain. (b) Dimeric C_H1-DDD2-Fab-veltuzumab, a Fab-DDD module with DDD2 fused to the carboxyl-terminal end of the F_d chain. (c) 22*-(20)-(20), a bsHexAb comprising C_k-AD2-IgG-epratuzumab and two dimeric C_H1-DDD2-Fab-veltuzumab modules. (d) 22-(20)-(20), a bsHexAb comprising C_H3-AD2-IgG-epratuzumab and two dimeric C_H1-DDD2-Fab-veltuzumab modules. (e) Dimeric IFNα2b-DDD2 module with DDD2 fused to the carboxyl-terminal end of IFNα2b via a flexible peptide linker. (f) 20*-2b, an immunocytokine with tetrameric IFNα2b constructed with C_k-AD2-IgG-veltuzumab fused with two dimeric IFNα2b-DDD2 modules. (g) 20-2b, an IgG-IFNα with tetrameric IFNα2b constructed with C_H3-AD2-IgG fused with two dimeric IFNα2b-DDD2 modules. Variable (V, blue or green) and constant (C, gray) domains of IgG heavy (H) and light (L) chains are represented as ovals. The DDD2 and AD2 peptides are shown as blue and yellow helices, respectively, with the locations indicated for the reactive sulfhydryl groups (SH) and the "locking" disulfide bridges indicated by red lines.

The DNL method also has been used to assemble Fc-based immunocytokines, comprising two or four molecules of interferon-alpha 2b (IFNα2b) fused to the C-terminal end of the C_H3-AD2-IgG Fc.[12−14] The Fc-IgG-IFNα maintained high specific activity, approaching that of recombinant IFNα, and were remarkably potent in vitro and in vivo against non-Hodgkin lymphoma (NHL) xenografts. The $T_{1/2}$ of the Fc-IgG-IFNα in mice was longer than that of PEGylated IFNα, but only half as long as the parental mAbs. Similar to the Fc-bsHexAbs, the Fc-IgG-IFNα dissociated in vivo over time and exhibited diminished CDC, but ADCC was enhanced.

We hypothesized that improving PK and in vivo stability might further enhance the in vivo efficacy of these already potent immunoconjugates. Using DNL, we generated a new class of IgG modules that have an AD2 peptide fused at the C-terminal end of the kappa light chain rather than the Fc, producing C_k-based (indicated by *) bsHexAbs and IgG-IFNα, for comparison with homologous Fc-based constructs. The C_k-IgG-IFNα, designated 20*-2b, has a similar molecular size and composition to its Fc-IgG-IFNα counterpart, 20-2b, each comprising veltuzumab and four copies of IFNα2b fused at the C-terminal ends of the light or heavy chains, respectively. The C_k-bsHexAb, designated 22*-(20)-(20), and its Fc-bsHexAb homologue, 22-(20)-(20), each comprise epratuzumab and four veltuzumab Fabs, which are fused at the C-terminal ends of the light and heavy chains, respectively. Compared to the analogous Fc-based immunoconjugates, the C_k-IgG-IFNα and C_k-bsHexAb were more stable in vivo, cleared more slowly from the circulation, and had improved Fc-effector function, significantly enhancing efficacy in vivo.

EXPERIMENTAL PROCEDURES

Antibodies and Cell Culture. Immunomedics, Inc., provided veltuzumab (anti-CD20 IgG1), epratuzumab (anti-CD22 IgG_1), a murine anti-IFNα mAb, hMN-14 (labetuzumab), a rat anti-idiotype mAb to veltuzumab (WR2), and a rat anti-idiotype mAb to epratuzumab (WN). HRP-conjugated second antibodies were from Jackson Immunoresearch (Westgrove, PA). Heat-inactivated fetal bovine serum (FBS) was obtained from Hyclone (Logan, UT). All other cell culture media and supplements were purchased from Invitrogen Life Technologies (Carlsbad, CA). SpESFX-10 cells[15] and production clones were maintained in H-SFM. Daudi was purchased from ATCC and grown in 10% FBS-RPMI (Manassas, VA).

DNL Constructs. For C_H3-AD2-IgG-veltuzumab, C_H3-AD2-IgG-epratuzumab, C_H1-DDD2-Fab-veltuzumab, and IFNα2b-DDD2, generation of the mammalian expression vectors and production clones and their use for the DNL conjugation of 20-2b and 22-(20)-(20) have been reported previously.[10,12,16,17] C_k-AD2-IgG was generated by recombinant engineering, whereby the AD2 peptide was fused to the C-terminal end of the kappa light chain (Figure 1a). Because the natural C-terminus of C_K is a cysteine residue, which forms a disulfide bridge to C_H1, a 16-amino-acid residue "hinge" linker was used to space the AD2 from the C_K-V_H1 disulfide bridge. The mammalian expression vectors for C_k-AD2-IgG-veltuzumab and C_k-AD2-IgG-epratuzumab were constructed using the pdHL2 vector, which was used previously for expression of the homologous C_H3-AD2-IgG modules. A 2208-bp nucleotide sequence was synthesized comprising the pdHL2 vector sequence ranging from the *Bam*HI restriction site within the V_K/C_K intron to the *Xho I* restriction site 3′ of the C_k intron, with the insertion of the coding sequence for the hinge linker (EFPKPSTPPGSSGGAP) and AD2 (CGQIEYLAKQIVD-

dx.doi.org/10.1021/bc300488f | *Bioconjugate Chem.* 2013, 24, 63−71

NAIQQAGC), in frame at the 3′-end of the coding sequence for C_K. This synthetic sequence was inserted into the IgG-pdHL2 expression vectors for veltuzumab and epratuzumab via *Bam*HI and *Xho I* restriction sites. Generation of production clones with SpESFX-10 was performed as described for the C_H3-AD2-IgG modules.[10,17] C_k-AD2-IgG-veltuzumab and C_k-AD2-IgG-epratuzumab were produced by stably transfected production clones in batch roller bottle culture, and purified from the supernatant fluid in a single step using MabSelect (GE Healthcare) Protein A affinity chromatography.

Following the same DNL process described previously for 22-(20)-(20),[10] C_k-AD2-IgG-epratuzumab was conjugated with C_H1-DDD2-Fab-veltuzumab (Figure 1b), a Fab-based module derived from veltuzumab, to generate the bsHexAb 22*-(20)-(20), where the 22* indicates the C_k-AD2 module of epratuzumab and each (20) symbolizes a stabilized dimer of veltuzumab Fab (Figure 1c). The properties of 22*-(20)-(20) were compared with those of 22-(20)-(20), the homologous Fc-bsHexAb comprising C_H3-AD2-IgG-epratuzumab (Figure 1d), which has similar composition and molecular size, but a different architecture.

Following the same DNL process described previously for 20-2b,[12] C_k-AD2-IgG-veltuzumab (Figure 1a) was conjugated with IFNα2b-DDD2, a module of IFNα2b with a DDD2 peptide fused at its C-terminal end (Figure 1e), to generate 20*-2b (Figure 1f), which comprises veltuzumab with a dimeric IFNα2b fused to each light chain. The properties of 20*-2b were compared with those of 20-2b (Figure 1g), which is the homologous Fc-IgG-IFNα.

For DNL conjugations, IgG-AD2 modules were mixed with a 10% mol excess of the appropriate DDD-module, and the DNL reaction was initiated with 1 mM reduced glutathione for 12−24 h at room temperature. Subsequently, 2 mM oxidized glutathione was added to the mixture, which was held at room temperature for an additional 12−24 h. Each of the bsHexAbs and IgG-IFNα was isolated from the DNL reaction mixture by MabSelect (Protein A) affinity chromatography.

Analytical Methods. Size-exclusion-HPLC was performed using an Alliance HPLC System with a BioSuite 250, 4 μm UHR SEC column (Waters Corp., Milford MA). SDS-PAGE was performed using 4−20% gradient Tris-glycine gels (Invitrogen, Gaithersburg, MD). IEF was performed at 1000 V, 20 mM, and 25 W for 1 h, using pH 6−10.5 Isogel Agarose IEF plates (Lonza, Basel, Switzerland) on a Bio-Phoresis horizontal electrophoresis cell (Bio-Rad, Hercules, CA). All colorimetric (ELISA and MTS) and fluorometric (CDC and ADCC) assays were quantified with an EnVision 2100 Multilabel Plate Reader (PerkinElmer, Waltham, MA).

Cell Binding. Binding to cells was measured by flow cytometry on a Guava PCA using *GuavaExpress* software (Millipore Corp., Billerica, MA). Veltuzumab and 20*-2b were labeled with phycoerythrin (PE) using a Zenon R-Phycoerythrin human IgG labeling kit following the manufacturer's protocol (Invitrogen, Molecular Probes). Daudi cells were incubated with the PE-veltuzumab and PE-20*-2b (0.1−15 nM) for 30 min at room temperature and washed with 1% BSA−PBS prior to analysis. Plots of concentration vs mean fluorescence intensity (MFI) were analyzed by linear regression.

In Vitro Cytotoxicity. Daudi human Burkitt lymphoma cells were plated at 10 000 cells/well in 96-well plates and incubated at 37 °C for 3 days in the presence of increasing concentrations of 20*-2b or 20-2b. Viable cell densities were determined using the MTS-based CellTiter 96 Cell Proliferation Assay (Promega, Madison, WI).

FcRn Binding Measurements. Neonatal Fc receptor (FcRn) binding was evaluated by surface plasmon resonance on a Biacore-X instrument (GE Healthcare) following the methods of Wang et al.[18] Soluble single-chain FcRn was generated following the methods of Feng et al.[19] The extracellular domain of the human FcRn heavy chain was fused with β2-microglobulin via a flexible peptide linker. The fusion protein was expressed using a modified pdHL2 vector in transfectant SpESFX-10 cells, and purified using Ni-Sepharose. Purified scFcRn was immobilized onto a CM5 biosensor chip using an amine coupling kit (GE Healthcare) to a density of ~600 response units (RU). The test articles were diluted with pH 6.0 running buffer [50 mM $NaPO_4$, 150 mM NaCl, and 0.05% (v/v) Surfactant 20] to 400, 200, 100, 50, and 25 nM and bound to the immobilized scFcRn for 3 min to reach equilibrium, followed by 2 min of dissociation with the flow rate at 30 μL/min. The sensorchip was regenerated with pH 7.5 running buffer between runs. To determine FcRn binding affinity (K_D) at pH 6.0, the data from all five concentrations were used simultaneously to fit a two-state reaction model (*BIAevaluation* software; GE Healthcare). Goodness of fit was indicated by χ^2 values.

PK Analyses. For measurement of intact and total (intact plus dissociated) IgG-IFNα, microtiter wells were adsorbed with WR2, a rat anti-Id for veltuzumab, at 5 μg/mL in 0.5 M Na_2CO_3, pH 9.5. Following blocking with 2% BSA−PBS, serum dilutions in antibody buffer (0.1% gelatin, 0.05% proclin, 0.05% Tween-20, 0.1 M NaCl, 0.1 M $NaPO_4$, pH 7.4) were incubated in the coated wells for 2 h. For measurement of intact IgG-IFNα, wells were probed with a mouse anti-IFNα mAb (5 μg/mL in antibody buffer) for 1 h, followed by detection with HRP-conjugated goat anti-mouse IgG-Fc. For measurement of total veltuzumab IgG, wells were probed with HRP-conjugated goat anti-human IgG-Fc for 1 h.

For measurement of intact and total bsHexAbs, microtiter wells were adsorbed with WN, a rat anti-idiotype for epratuzumab. Serum dilutions were incubated in the coated wells for 2 h. For detection of intact bsHexAb, wells were probed with HRP-conjugated WR2 (1 μg/mL in antibody buffer) for 1 h. For detection of total epratuzumab IgG, wells were probed with HRP-conjugated goat anti-human IgG-Fc for 1 h.

Signal was developed with *o*-phenylenediamine dihydrochloride substrate solution and OD was measured at 490 nM. The concentrations of intact and total species were extrapolated from construct-specific standard curves. PK was analyzed using the *WinNonLin* PK software package (v 5.1; Pharsight Corp.; Mountain View, CA).

In Vivo and Ex Vivo Methods. All studies in mice were approved by the UMDNJ Institutional Animal Care and Use Committee (IACUC), and performed in accordance with the AAALAC, USDA, and DHHS regulations. Injection and collection of sera from rabbits was performed by Lampire Biological Laboraories (Pipersville, PA) under their in-house IACUC approval. For PK studies, 10-week-old male Swiss-Webster mice (Taconic, Germantown, NY) and New Zealand White rabbits were injected subcutaneously (SC), and also intravenously (IV) for mice, with test agents diluted in PBS. Blood samples were obtained by cardiac puncture and from the ear vein for mice and rabbits, respectively. Serum was isolated

dx.doi.org/10.1021/bc300488f | *Bioconjugate Chem.* 2013, 24, 63−71

from clotted blood by centrifugation and diluted in antibody buffer, prior to analysis by ELISA.

Human blood specimens were collected from healthy volunteer donors under a protocol approved by the New England Institutional Review Board (Wellesley, MA). In vitro ADCC and CDC activity was assayed as described previously.[17] For ADCC, Daudi cells were incubated for 4 h at 37 °C with PBMCs, which were isolated from the blood of healthy donors, at a 50:1 effector/target ratio using test agents at 33 nM.

In Vivo Efficacy in Mice. Female 8−12-week old C.B.17 homozygous SCID mice (Taconic) were inoculated IV with 1.5 × 10^7 Daudi cells on day 0. For comparison of the bsHexAbs, treatment was administered by SC injection on days 1 and 5. For comparison of the IgG-IFNα, treatments were administered as a single SC injection on day 7. Saline was used as a control treatment. Animals, monitored daily, were humanely euthanized when hind-limb paralysis developed or if they became otherwise moribund. Additionally, mice were euthanized if they lost more than 15% of initial body weight. Survival curves were analyzed using Kaplan−Meier plots, using the *Prism* v 4.03 software package (GraphPad Software, Inc., San Diego, CA). Some outliers determined by critical Z test were censored from analyses.

Statistical Analyses. Statistical significance ($P < 0.05$) was determined using Student's *t* tests for all results except for the in vivo survival curves, which were evaluated by log-rank analysis.

RESULTS

Synthesis of C_k-Based Immunoconjugates. For each DNL conjugation, the specific IgG-AD2 module was combined with a 10% mol excess of the specific dimeric DDD-module, which binds in a 2:1 stoichiometric ratio with the former. For example, 18 mg C_k-AD2-IgG-epratuzumab (MW = 155 kDa) mixed with 28 mg of C_H1-DDD2-Fab-veltuzumab (MW = 108 × 2 = 216 kDa) yielded 37 mg of 22*-(22)-(22), which is 86% of the theoretical yield. Combining 195 mg of C_k-AD2-IgG-hA20 with 150 mg of IFNα2b-DDD2 (MW = 52 × 2 = 104 kDa) generated 283 mg of 20*-2b, which is 87% of the theoretical yield. DNL conjugation produced homogeneous preparations of 22*-(20)-(20), 22-(20)-(20), 20*-2b, and 20-2b, which were each isolated by Protein A affinity chromatography. As shown by SDS-PAGE (nonreducing), each conjugate was resolved into a tight cluster of bands with relative mobility conforming to their expected size (SI Figure S1a), and under reducing conditions, only bands representing the constituent polypeptides for each conjugate were evident, demonstrating a high degree of purity (SI Figure S1b−d). For each conjugate, SE-HPLC resolved a major peak having a retention time consistent with their molecular size (SI Figures S2 and S3). The longer retention times observed for 22*-(20)-(20) and 20*-2b are likely due to their more compact structure, as compared to 22-(20)-(20) and 20-2b, respectively. Isoelectric focusing showed that 20*-2b and 20-2b have a similar pI (calculated pI = pH 7.22), with no evidence of unreacted IgG-AD2 (pI = pH 7.86) or IFNα2b-DDD2 (pI = pH 6.87) modules (SI Figure S4).

Both conjugates retain full binding of the parental mAbs. The 22*-(20)-(20) exhibited similar binding to veltuzumab, which is higher than that of epratuzumab, because CD20 is expressed at a higher level than CD22 on Daudi (SI Figure S5a). 20*-2b exhibited identical binding to veltuzumab on live Daudi cells (SI Figure S5b). Cytotoxicity also was similar between the C_k and Fc versions in Daudi cells (EC_{50} = 0.2 pM), demonstrating equivalent CD20 binding and IFNα specific activity (SI Figure S6).

Pharmacokinetics. We reported previously that the $T_{1/2}$ values for Fc-bsHexAbs were approximately half as long as those of their parental mAbs in mice.[10] In the initial study, which measured the serum concentrations of 22*-(20)-(20), 22-(20)-(20), and epratuzumab in mice over a period of 72 h after subcutaneous (SC) injection (Figure 2a), 22-(20)-(20)

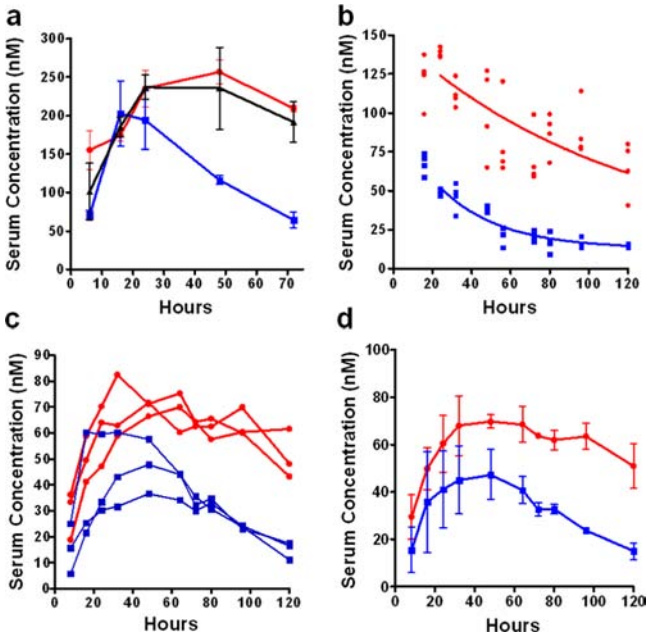

Figure 2. Pharmacokinetics of 22*-(20)-(20) and 22-(20)-(20) in mice and rabbits. At the indicated intervals, the concentration of the intact molecules in serum samples was measured using a bispecific ELISA. Animals were administered 22*-(20)-(20) (red circle/line), 22-(20)-(20) (blue square/line), or epratuzumab (black triangle/line) subcutaneously. Mice were terminally bled, while rabbits were serially bled. (a) Groups of 3 mice (mean ± SD) were dosed with 1.0 mg of bsHexAb or an equal molar amount of epratuzumab (0.41 mg). (b) Groups of 4 mice were dosed with 0.5 mg of bsAb. Individual data points are plotted with nonlinear regression analysis using a one-phase exponential decay model with *Prism* software. (c,d) Rabbits were administered 18 mg (6 mg/kg) of bsAb. The PK curves are shown for the individual animals (c) and the mean ± SD of each group (d).

reached maximal concentration at 16 h and was cleared with a $T_{1/2}$ of about 1 day, similar to the findings before. In comparison, both epratuzumab and 22*-(20)-(20) reached peak levels between 24 and 48 h, while clearing similarly, but more slowly than 22-(20)-(20). A subsequent study monitoring clearance over 5 days again found 22*-(20)-(20) with superior PK, showing ~2-fold higher maximum concentration in serum, with longer $T_{1/2}$ and mean residence time (MRT), culminating in a 3.8-fold greater area under the curve (AUC) (Figure 2b; Table 1).

As in mice, the PK parameters determined in rabbits were ~2-fold greater for 22*-(20)-(20), resulting in a 3.3-fold greater AUC, compared to 22-(20)-(20) (Figure 2c,d; Table 1). Importantly, the concentrations of the 22*-(20)-(20) following SC administration in both mice and rabbits were sustained for longer periods.

Binding affinity (K_D) of the bsHexAbs to FcRn was assessed by surface plasmon resonance and found to be 166 and 310 nM

dx.doi.org/10.1021/bc300488f | *Bioconjugate Chem.* 2013, 24, 63−71

Table 1. Summary of Pharmacokinetic Parameters[a]

species	route	dose (mg)	construct	$T_{1/2}$ (h)	T_{max} (h)	C_{max} (μg/mL)	AUC (0−∞) (h*mg/mL)	MRT (h)
mouse	IV	1.0	20*-2b	36	6	649	32	55
			20-2b	17	6	630	16	19
mouse	SC	1.0	20*-2b	38	16	312	18	62
			20-2b	16	16	146	7	30
mouse	SC	0.5	22*-(20)-(20)	107	24	51	7	153
			22-(20)-(20)	55	16	27	2	85
rabbit	SC	18	22*-(20)-(20)	118	53	32	6	179
			22-(20)-(20)	51	37	18	2	89

[a] $T_{1/2}$, elimination half-life; T_{max}, time of maximal concentration; C_{max}, maximal concentration; AUC, area under the curve; MRT, mean residence time.

for 22*-(20)-(20) and 22-(20)-(20), respectively (P = 0.01). The affinity of epratuzumab (16 nM) was approximately 10-fold stronger than that of 22*-(20)-(20) (P = 0.007) (SI Figure S7 and Table S1).

Fc-IgG-IFNα constructs, such as 20-2b, also were cleared from the circulation more rapidly than their parental mAb.[12] However, when the PK parameters of 20*-2b and 20-2b following either SC or IV injection were compared (Figure 3), the $T_{1/2}$, C_{max}, and MRT were each again about 2-fold higher for 20*-2b, resulting in a 2.8-fold greater AUC, compared to 20-2b (Table 1). For IV administration, 20*-2b had a 2- and 2.8-fold longer $T_{1/2}$ and MRT, respectively, and a 2-fold greater AUC.

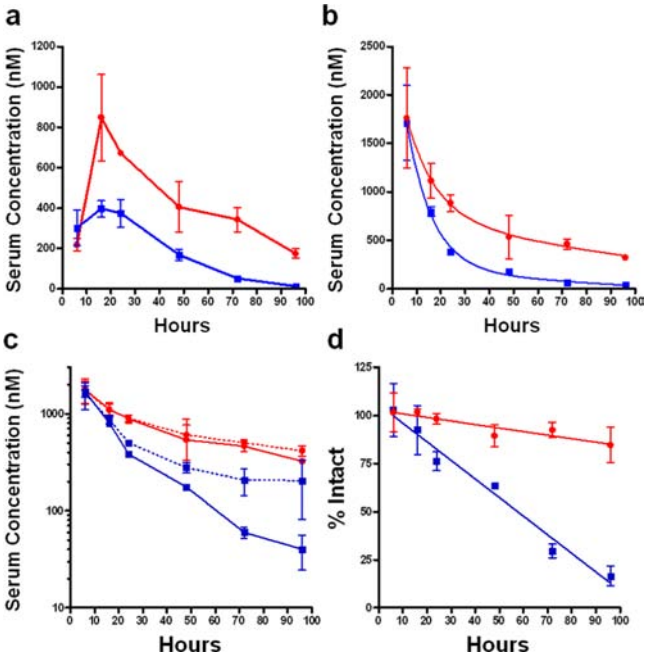

Figure 3. Pharmacokinetics and in vivo stability of 20*-2b and 20-2b in mice. Groups of 3 mice were administered 1.0 mg of 20*-2b (red circle/line) or 20-2b (blue square/line) by subcutaneous (a) or intravenous (b,c,d) injection. (c) For each data point, obtained from individual animals, the serum concentration of the intact IgG-IFNα and total IgG (veltuzumab) was measured using bispecific (solid line) or veltuzumab-specific (dashed line) ELISA formats. (d) For each data point, the % intact IgG-IFNα was calculated by dividing the serum concentration measured with the bispecific ELISA by that determined with the veltuzumab-specific assay, and multiplying the quotient by 100. The % intact IgG-IFNα was plotted vs hours post injection, and the dissociation rate was determined by linear regression analysis. Each plot shows the mean values ±SD.

In Vivo Stability. The Fc-bsHexAbs and Fc-IgG-IFNα are stable ex vivo in serum.[10,12] However, analysis of serum samples from earlier PK studies suggested that these constructs do dissociate in vivo over time, presumably by intracellular processing. We compared the in vivo stability of 20*-2b and 20-2b by measuring the concentrations of the intact IgG-IFNα and the total veltuzumab, which allowed differentiation of the intact from the dissociated species (Figure 3c). The % intact IgG-IFNα was plotted versus time (Figure 3d), and in vivo dissociation rates for 20-2b and 20*-2b were calculated by linear regression to 0.97%/h and 0.18%/h, respectively. A similar analysis was performed on serum samples following SC injection of the bsHexAbs in mice, with in vivo dissociation rates for 22-(20)-(20) and 22*-(20)-(20) calculated to 0.55%/h and 0.19%/h, respectively (SI Figure S8). Interestingly, both 22-(20)-(20) and 22*-(20)-(20) were completely stable in vivo following SC injections in rabbits (SI Figure S9).

Effector Function. We reported that Fc-IgG-IFNα and Fc-bsHexAbs did not induce measurable CDC in vitro, even when their parental mAb had potent activity.[10,12] Consistent with prior results, veltuzumab exhibited strong CDC, yet no activity was evident for 20-2b (Figure 4a); but, surprisingly, 20*-2b induced strong CDC, which approached the potency of veltuzumab. Under these in vitro conditions, epratuzumab lacked CDC, whereas 22-(20)-(20) achieved a modest increase, and 22*-(20)-(20) induced even greater activity, which was ~10-fold less potent than veltuzumab (Figure 4b).

Unlike CDC, the Fc-based conjugates did not have reduced ADCC, but instead, 20-2b exhibited enhanced ADCC compared to veltuzumab.[12] Depending on the PBMC donor, epratuzumab induced little or no ADCC in vitro, and not surprisingly, 22-(20)-(20) did not show statistically significant improvement (Figure 4c). However, the ADCC associated with 22*-(20)-(20) was not significantly different from that of veltuzumab, when PBMCs of a high-ADCC donor were used (Figure 4c). With a low-ADCC PBMC donor, 22*-(20)-(20) had enhanced activity (11.4% lysis), compared to that of epratuzumab (2.3%) and 22-(20)-(20) (4.3%), but it was lower than that of veltuzumab (18.5%) (P = 0.0326, data not shown).

In Vivo Efficacy. As reported previously, 20-2b is remarkably potent in treating mice bearing human Daudi Burkitt lymphoma xenografts, which are highly sensitive to direct killing by IFNα.[12] Using the same model, the C_k-based conjugates demonstrated even more potent antitumor activity than their Fc-based counterparts (Figure 5a). While both 20-2b and 20*-2b at a single 1 μg dose cured the majority of the animals, with a median survival time (MST) greater than 189

dx.doi.org/10.1021/bc300488f | Bioconjugate Chem. 2013, 24, 63−71

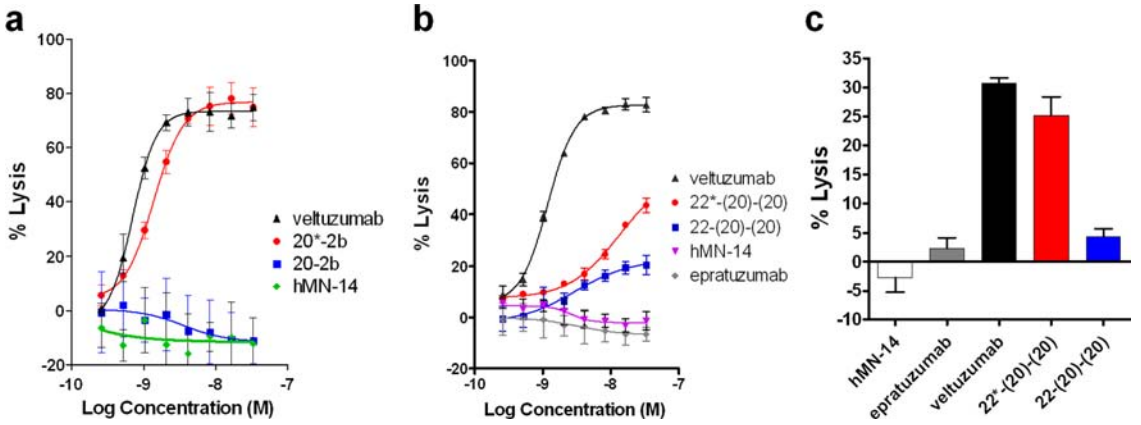

Figure 4. Effector functions. In vitro CDC was compared among (a) 20*-2b, 20-2b, and veltuzumab, and (b) 22*-(20)-(20), 22-(20)-(20), veltuzumab, and epratuzumab. (c) In vitro ADCC was compared among 22*-(20)-(20), 22-(20)-(20), veltuzumab, and epratuzumab at 33 nM. mAb hMN-14 was used as a nonbinding isotype control for each experiment.

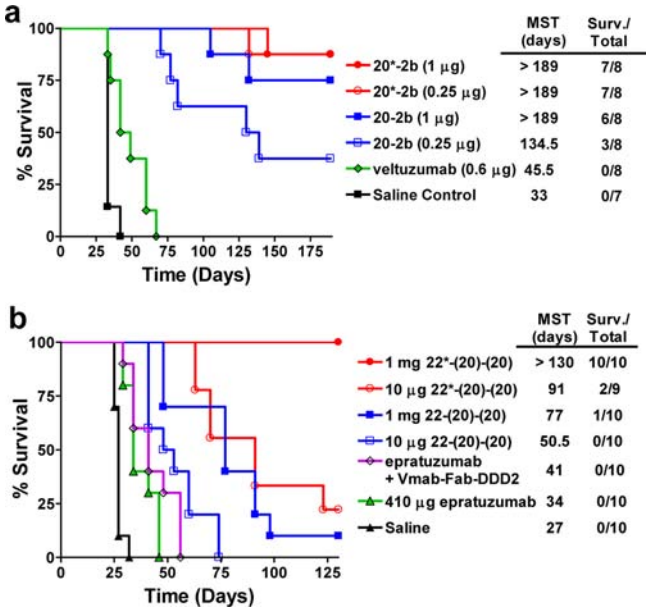

Figure 5. In vivo efficacy with disseminated Daudi Burkitt lymphoma xenografts. (a) Groups of 8 SCID mice were inoculated with Daudi by IV injection. On day 7, mice were administered a single dose of 1.0 or 0.25 μg of 20*-2b (red) or 20-2b (blue) by SC injection. Control groups were administered 0.6 μg of veltuzumab or saline (black). (b) Groups of 10 SCID mice were inoculated by IV injection on day 0. On days 1 and 5, mice were administered high (1 mg) or low (10 μg) doses of 22*-(20)-(20) (red) or 22-(20)-(20) (blue) by SC injection. Control groups were administered a high dose of epratuzumab (green) and a high dose epratuzumab plus C_H1-DDD2-veltuzumab (purple) or saline (black). Statistical significance was determined by log-rank analysis of Kaplan–Myer survival plots.

days, 20*2b, but not 20-2b, at 0.25 μg maintained its potency, providing evidence of significantly improved therapeutic efficacy (MST > 189 days with 7/8 cures for 20*2b vs 134.5 days with just 3/8 survivors for 20-2b; P = 0.0351). A molar equivalent of veltuzumab (0.6 μg) to 1 μg of 20-2b increased the MST by only 12.5 days over saline control. The superiority of another different C_k construct over the Fc-parental construct was shown again in the disseminated Daudi model, where animals were administered two injections (days 1 and 5) of high (1 mg) or low (10 μg) doses of 22*-(20)-(20) or 22-(20)-(20) (Figure 5b). For the high dose, the MST was >130 and 71 days with 100% and 10% survival for 22*-(20)-(20) and 22-(20-(20), respectively (P < 0.0001). With the low-dose treatment, the MST was 91 days for 22*-(20)-(20) with two mice surviving, compared to 50.5 days for 22-(20-(20) with no survivors (P = 0.0014). High doses of each bsHexAb improved survival significantly more (P < 0.0001) than epratuzumab either alone or in combination with C_H1-DDD2-Fab-veltuzumab, which was given at a molar equivalent to the 1 mg dose of bsHexAb. At the 100-fold lower dosing, both bsHexAbs were superior to high-dose epratuzumab (P < 0.003), and 22*-(20)-(20), but not 22-(20)-(20), was superior to high-dose epratuzumab plus C_H1-DDD2-Fab-veltuzumab (P < 0.0001).

DISCUSSION

The various formats of antibody-based fusion proteins, including bsAbs[1] and immunocytokines,[20] can largely be categorized into three groups, based on where additional moieties are fused to a whole IgG, an Fc, or an antigen-binding fragment, such as Fab, scFv, or diabody. Whereas Fc-fusion may increase $T_{1/2}$, and fusion to antigen-binding fragments should impart targeting, only fusion to IgG could be expected to achieve antibody targeting, full Fc effector function, and markedly extended PK. Because not all IgG-fusion designs are created equal, effector activities and PK are known to vary widely among the different formats and even between particular constructs of the same design.

The DNL method is exceptional in generating immunoconjugates that retain full antigen-binding avidity of the targeting antibody and biological activity of the appending effector molecules (e.g., cytokines) and have potent efficacy both in vitro and in vivo.[3,10,12−14] However, Fc-bsHexAbs and Fc-IgG-IFNα were cleared from the circulation at approximately twice the rate of their parental mAbs. Suboptimal PK is a common deficiency associated with immunoconjugates that is primarily attributed to impaired dynamic binding to the FcRn.[2] To improve PK, we engineered a new class of IgG-AD2 module having the AD2 peptide fused at the C-terminal end of the light chain. The new modules were used to assemble C_k-bsHexAbs and C_k-IgG-IFNα, which not only exhibited comparable in vitro properties to those of their Fc-based homologues, including antigen binding, IFNα specific activity, and in vitro cytotoxicity, but also had superior PK, in vivo stability, and Fc effector

dx.doi.org/10.1021/bc300488f | Bioconjugate Chem. 2013, 24, 63−71

activity, which together resulted in increased in vivo efficacy, compared to the already potent Fc-based counterparts.

The superior PK of the C_k-bsHexAbs and C_k-IgG-IFNα is most likely attributed to their increased binding affinity to the FcRn, which was twice as strong at pH 6.0 for 22*-(20)-(20) compared to 22-(20)-(20). This is not surprising, because FcRn binding is mediated by portions of the C_H2 and C_H3 domains of IgG, with critical contact sites located near the C-terminal end of the Fc.[21,22] Considering that the $T_{1/2}$ of 22*-(20)-(20) was in the range of epratuzumab,[10] it was unanticipated that FcRn binding was approximately 10-fold weaker for the former (155 nM). However, using this same method, we measured the FcRn K_D at 42 and 92 nM for other humanized mAbs, which typically have PK similar to epratuzumab (data not shown). $T_{1/2}$ is not necessarily directly correlated with FcRn K_D at pH 6.0.[23,24] It has been suggested that the rate of dissociation at pH 7.4 is equally or perhaps more important in determining $T_{1/2}$.[18] Although FcRn:IgG contacts are limited to the Fc domain, the antigen-binding domain can negatively impact FcRn binding, as evidenced by the fact that most therapeutic antibodies share a very similar Fc (IgG_1), yet vary widely in FcRn K_D and $T_{1/2}$.[25] Additional factors include endocytosis, ligand/antibody ratio, antibody structural stability, antibody pI, and methionine oxidation.[2]

For fusion proteins, the FcRn K_D and $T_{1/2}$ can be influenced by the nature and location of the fusion partner.[25,26] We observed that the $T_{1/2}$ of each IgG-IFNα was shorter than the corresponding bsHexAb that was assembled using the same class of IgG-AD2 module. For example, the $T_{1/2}$ of 20*-2b (37.9 h) was markedly shorter than that of 22*-(20)-(20) (106.5 h), suggesting that, independent of their location, the IFNα groups negatively impact FcRn binding, perhaps by lowering the pI of the adduct.

We have identified the C-terminal end of the light chain as the most advantageous location for fusion to IgG. An immunocytokine of single-chain IL-12 fused to the N-terminal end of the heavy chain of an anti-HER2 IgG_3 retained HER2 binding.[27] We applied a similar strategy using DNL by constructing an IgG-AD2 module having the AD2 peptide fused to the N-terminal end of the veltuzumab heavy chain. However, bsHexAbs and IgG-IFNα made with this module did not bind CD20 on cells (data not shown). This might have been because of the large size of the additional $(Fab)_2$ or $(IFN\alpha2b)_2$ groups. That these conjugates bound to anti-idiotype mAbs suggests that the nature of the antigen, which is a small extracellular loop of CD20, might be a factor. The C-terminal end of the heavy chain is the most common and convenient location for fusion to IgG.[20] However, this also is the most likely location to impact FcRn binding and PK negatively. For example, an immunocytokine of GM-CSF fused at the C-terminus of the heavy chain of an anti-HER2 IgG_3 exhibited markedly reduced $T_{1/2}$ (10 h) compared to the parental mAb (110 h).[28] Fc-based bsAbs also suffer from diminished PK. As an example, a bsAb having an anti-IGF-1R scFv fused to the C-terminal end of the heavy chain of an anti-EGFR IgG cleared from circulation in mice twice as fast ($T_{1/2}$ = 9.93 h), compared to the parental mAb ($T_{1/2}$ = 20.36 h).[29]

Croasdale and colleagues systematically studied the effect of fusion location with IgG-scFv tetravalent bsAbs using an anti-IGF-1R IgG_1 fused at the N- or C-termini of the heavy or light chains, with an anti-EGFR scFv.[30] Their results support our conclusion that the C-terminus of the light chain is the most favorable fusion location for IgG-based immunoconjugates, since this format was produced at the highest yield, had the longest $T_{1/2}$, and was the most effective in vivo. The authors indicated that each construct bound FcRn and FcγRIIIa; however, K_D was not reported. Among the different formats, the C-terminal heavy chain fusion had the shortest $T_{1/2}$. Fusion at the N- or C-terminus of the heavy chain resulted in substantially reduced or complete loss, respectively, of ADCC. Alternatively, fusion at the C-terminus of the light chain did not decrease ADCC. Our results show that fusion location can impact ADCC. For the bsHexAbs comprising epratuzumab as the IgG, which has minimal ADCC, strong ADCC was measured for 22*-(20)-(20), but not 22-(20)-(20), suggesting that this Fc effector function was provided by the addition of the four anti-CD20 Fabs, and that their fusion location is critical. Additionally, 22*-(20)-(20) showed moderate CDC, which was not detected for epratuzumab, and only modestly increased for 22-(20)-(20), suggesting that this effector function also can be bestowed to a CDC-lacking mAb by the addition of Fabs of a CDC-inducing mAb, and that the activity is sensitive to the location of the fusion site. This was demonstrated clearly with the IgG-IFNα, where the Fc-IgG-IFN, 20-2b, did not have detectable CDC and 20*-2b induced potent activity, similar to veltuzumab.

Although the Fc-bsHexAbs and Fc-IgG-IFNα are quite stable in human or mouse sera and whole blood,[10,12] the Fc-fusions, in particular, were not completely stable in vivo. The Fc-based conjugates dissociated at a rate of 0.5−1.0%/h in mice, compared to <0.2%/h for the C_k-based constructs. Because dissociation has never been observed ex vivo, we presume it occurs by an intracellular process. Interestingly, there was no evidence of in vivo instability in rabbits, even after 5 days, and thus, we cannot predict from the current set of data how the constructs will be handled in humans. The C-terminal lysine residue of the heavy chain is often cleaved proteolytically during antibody production. The common Fc-based fusion proteins, where additional groups are fused to the C-terminal lysine, potentially can be cleaved in vivo by proteases, such as plasmin, which cleave after exposed lysine residues.[31]

In summary, this study demonstrates the superior in vivo properties of bsAbs and immunocytokines made using the DNL method with fusion at the C-terminal end of the light chain, suggesting that the C-terminus of the light chain would be the preferred fusion location for most immunoconjugates with intended clinical use.

■ ASSOCIATED CONTENT

Supporting Information

Figures S1−S9, Table S1. This material is available free of charge via the Internet at http://pubs.acs.org.

■ AUTHOR INFORMATION

Corresponding Author

*E-mail: Erossi@immunomedics.com; Phone: 973-605-8200; Fax: 973-605-1340.

Notes

The authors declare the following competing financial interest(s): All authors are employees or hold stock of Immunomedics, Inc.

■ ACKNOWLEDGMENTS

We thank Roberto Arrojo for experimental expertise in ADCC and Biacore experiments; Rongxiu Li, Preeti Trisal, and Dion

Yeldell for their efforts with PK analyses; John Kopinski and Diana Chereches for protein production, purification, and characterization, Maria Zalath and Anju Nair for their contribution with animal studies; and Robert M. Sharkey, Ph.D., for critical analysis of results and editing of the manuscript.

■ ABBREVIATIONS

20-2b, immunocytokine comprising 4 IFNα moieties fused at the C-terminal ends of the heavy chains of veltuzumab; 20*-2b, immunocytokine comprising 4 IFNα moieties fused at the C-terminal ends of the light chains of veltuzumab; 22-(20)-(20), bispecific hexavalent antibody comprising 4 Fabs of veltuzumab fused to the C-terminal ends of the heavy chains of epratuzumab; 22*-(20)-(20), bispecific hexavalent antibody comprising 4 Fabs of veltuzumab fused to the C-terminal ends of the light chains of epratuzumab; AD, anchor domain; ADCC, antibody-dependent cellular cytotoxicity; AUC, area under the curve; bsHexAb, bispecific hexavalent antibody; CDC, complement-dependent cytotoxicity; C_k-bsHexAb, bispecific hexavalent antibody having 4 Fabs fused to the C-terminal ends of the light chains of an IgG; C_k-IgG-IFNα, immunocytokine having 4 IFNα fused to the C-terminal ends of the light chains of an IgG; DDD, dimerization and docking domain; DNL, dock-and-lock; Fc-bsHexAb, bispecific hexavalent antibody having 4 Fabs fused to the C-terminal ends of the heavy chains of an IgG; Fc-IgG-IFNα, immunocytokine having 4 IFNα fused to the C-terminal ends of the heavy chains of an IgG; FcRn, neonatal Fc receptor; IEF, isoelectric focusing; IFNα, interferon-alpha; IgG-IFNα, immunocytokine comprising an IgG and IFNα; IV, intravenous; K_D, dissociation constant; mAb, monoclonal antibody; MST, median survival time; PBMC, peripheral blood mononuclear cells; PK, pharmacokinetics; SC, subcutaneous; scFv, single-chain Fv fragment; $T_{1/2}$, circulating serum half-life.

■ REFERENCES

(1) Kontermann, R. E. (2010) Alternative antibody formats. *Curr. Opin. Mol. Ther. 12*, 176−183.
(2) Kuo, T. T., and Aveson, V. G. (2011) Neonatal Fc receptor and IgG-based therapeutics. *MAbs 3*, 422−430.
(3) Rossi, E. A., Goldenberg, D. M., and Chang, C. H. (2012) The dock-and-lock method combines recombinant engineering with site-specific covalent conjugation to generate multifunctional structures. *Bioconjugate Chem. 23*, 309−323.
(4) Baillie, G. S., Scott, J. D., and Houslay, M. D. (2005) Compartmentalisation of phosphodiesterases and protein kinase A: opposites attract. *FEBS Lett. 579*, 3264−3270.
(5) Wong, W., and Scott, J. D. (2004) AKAP signalling complexes: focal points in space and time. *Nat. Rev. Mol. Cell Biol. 5*, 959−970.
(6) Carr, D. W., Stofko-Hahn, R. E., Fraser, I. D., Bishop, S. M., Acott, T. S., Brennan, R. G., and Scott, J. D. (1991) Interaction of the regulatory subunit (RII) of cAMP-dependent protein kinase with RII-anchoring proteins occurs through an amphipathic helix binding motif. *J. Biol. Chem. 266*, 14188−14192.
(7) Colledge, M., and Scott, J. D. (1999) AKAPs: from structure to function. *Trends Cell Biol. 9*, 216−221.
(8) Newlon, M. G., Roy, M., Morikis, D., Hausken, Z. E., Coghlan, V., Scott, J. D., and Jennings, P. A. (1999) The molecular basis for protein kinase A anchoring revealed by solution NMR. *Nat. Struct. Biol. 6*, 222−227.
(9) Newlon, M. G., Roy, M., Morikis, D., Carr, D. W., Westphal, R., Scott, J. D., and Jennings, P. A. (2001) A novel mechanism of PKA anchoring revealed by solution structures of anchoring complexes. *EMBO J. 20*, 1651−1662.
(10) Rossi, E. A., Goldenberg, D. M., Cardillo, T. M., Stein, R., and Chang, C. H. (2009) Hexavalent bispecific antibodies represent a new class of anticancer therapeutics: 1. Properties of anti-CD20/CD22 antibodies in lymphoma. *Blood 113*, 6161−6171.
(11) Gupta, P., Goldenberg, D. M., Rossi, E. A., and Chang, C. H. (2010) Multiple signaling pathways induced by hexavalent, monospecific, anti-CD20 and hexavalent, bispecific, anti-CD20/CD22 humanized antibodies correlate with enhanced toxicity to B-cell lymphomas and leukemias. *Blood 116*, 3258−3267.
(12) Rossi, E. A., Goldenberg, D. M., Cardillo, T. M., Stein, R., and Chang, C. H. (2009) CD20-targeted tetrameric interferon-alpha, a novel and potent immunocytokine for the therapy of B-cell lymphomas. *Blood 114*, 3864−3871.
(13) Rossi, E. A., Rossi, D. L., Stein, R., Goldenberg, D. M., and Chang, C. H. (2010) A bispecific antibody-IFNalpha2b immunocytokine targeting CD20 and HLA-DR is highly toxic to human lymphoma and multiple myeloma cells. *Cancer Res. 70*, 7600−7609.
(14) Rossi, E. A., Rossi, D. L., Cardillo, T. M., Stein, R., Goldenberg, D. M., and Chang, C. H. (2011) Preclinical studies on targeted delivery of multiple IFN{alpha}2b to HLA-DR in diverse hematologic cancers. *Blood 118*, 1877−1884.
(15) Rossi, D. L., Rossi, E. A., Goldenberg, D. M., and Chang, C. H. (2011) A new mammalian host cell with enhanced survival enables completely serum-free development of high-level protein production cell lines. *Biotechnol. Prog. 27*, 766−775.
(16) Chang, C. H., Rossi, E. A., Cardillo, T. M., Nordstrom, D. L., McBride, W. J., and Goldenberg, D. M. (2009) A new method to produce monoPEGylated dimeric cytokines shown with human interferon-alpha2b. *Bioconjugate Chem. 20*, 1899−1907.
(17) Rossi, E. A., Goldenberg, D. M., Cardillo, T. M., Stein, R., Wang, Y., and Chang, C. H. (2008) Novel designs of multivalent anti-CD20 humanized antibodies as improved lymphoma therapeutics. *Cancer Res. 68*, 8384−8392.
(18) Wang, W., Lu, P., Fang, Y., Hamuro, L., Pittman, T., Carr, B., Hochman, J., and Prueksaritanont, T. (2011) Monoclonal antibodies with identical Fc sequences can bind to FcRn differentially with pharmacokinetic consequences. *Drug Metab. Dispos. 39*, 1469−1477.
(19) Feng, Y., Gong, R., and Dimitrov, D. S. (2011) Design, expression and characterization of a soluble single-chain functional human neonatal Fc receptor. *Protein Expr. Purif. 79*, 66−71.
(20) Kontermann, R. E. (2012) Antibody-cytokine fusion proteins. *Arch. Biochem. Biophys. 526*, 194−205.
(21) Huber, A. H., Kelley, R. F., Gastinel, L. N., and Bjorkman, P. J. (1993) Crystallization and stoichiometry of binding of a complex between a rat intestinal Fc receptor and Fc. *J. Mol. Biol. 230*, 1077−1083.
(22) Raghavan, M., Chen, M. Y., Gastinel, L. N., and Bjorkman, P. J. (1994) Investigation of the interaction between the class I MHC-related Fc receptor and its immunoglobulin G ligand. *Immunity 1*, 303−315.
(23) Dall'Acqua, W. F., Woods, R. M., Ward, E. S., Palaszynski, S. R., Patel, N. K., Brewah, Y. A., Wu, H., Kiener, P. A., and Langermann, S. (2002) Increasing the affinity of a human IgG1 for the neonatal Fc receptor: biological consequences. *J. Immunol. 169*, 5171−5180.
(24) Gurbaxani, B., la Cruz, L. L., Chintalacharuvu, K., and Morrison, S. L. (2006) Analysis of a family of antibodies with different half-lives in mice fails to find a correlation between affinity for FcRn and serum half-life. *Mol. Immunol. 43*, 1462−1473.
(25) Suzuki, T., Ishii-Watabe, A., Tada, M., Kobayashi, T., Kanayasu-Toyoda, T., Kawanishi, T., and Yamaguchi, T. (2010) Importance of neonatal FcR in regulating the serum half-life of therapeutic proteins containing the Fc domain of human IgG1: a comparative study of the affinity of monoclonal antibodies and Fc-fusion proteins to human neonatal FcR. *J. Immunol. 184*, 1968−1976.
(26) Lee, H., Kimko, H. C., Rogge, M., Wang, D., Nestorov, I., and Peck, C. C. (2003) Population pharmacokinetic and pharmacodynamic modeling of etanercept using logistic regression analysis. *Clin. Pharmacol. Ther. 73*, 348−365.

(27) Peng, L. S., Penichet, M. L., and Morrison, S. L. (1999) A single-chain IL-12 IgG3 antibody fusion protein retains antibody specificity and IL-12 bioactivity and demonstrates antitumor activity. *J. Immunol. 163*, 250−258.
(28) Dela Cruz, J. S., Trinh, K. R., Morrison, S. L., and Penichet, M. L. (2000) Recombinant anti-human HER2/neu IgG3-(GM-CSF) fusion protein retains antigen specificity and cytokine function and demonstrates antitumor activity. *J. Immunol. 165*, 5112−5121.
(29) Dong, J., Sereno, A., Aivazian, D., Langley, E., Miller, B. R., Snyder, W. B., Chan, E., Cantele, M., Morena, R., Joseph, I. B., Boccia, A., Virata, C., Gamez, J., Yco, G., Favis, M., Wu, X., Graff, C. P., Wang, Q., Rohde, E., Rennard, R., Berquist, L., Huang, F., Zhang, Y., Gao, S. X., Ho, S. N., Demarest, S. J., Reff, M. E., Hariharan, K., and Glaser, S. M. (2011) A stable IgG-like bispecific antibody targeting the epidermal growth factor receptor and the type I insulin-like growth factor receptor demonstrates superior anti-tumor activity. *MAbs 3*, 273−288.
(30) Croasdale, R., Wartha, K., Schanzer, J. M., Kuenkele, K. P., Ries, C., Mayer, K., Gassner, C., Wagner, M., Dimoudis, N., Herter, S., Jaeger, C., Ferrara, C., Hoffmann, E., Kling, L., Lau, W., Staack, R. F., Heinrich, J., Scheuer, W., Stracke, J., Gerdes, C., Brinkmann, U., Umana, P., and Klein, C. (2012) Development of tetravalent IgG1 dual targeting IGF-1R-EGFR antibodies with potent tumor inhibition. *Arch. Biochem. Biophys. 526*, 206−218.
(31) Gillies, S. D., Reilly, E. B., Lo, K. M., and Reisfeld, R. A. (1992) Antibody-targeted interleukin 2 stimulates T-cell killing of autologous tumor cells. *Proc. Natl. Acad. Sci. U. S. A. 89*, 1428−1432.